applied sciences

MDPI

Article

Bearing Capacity of Shallow Foundations on Unsaturated Silty Soils

Mehmet Ugur Yilmazoglu [1,*] and Askin Ozocak [2]

1 Institute of Natural Sciences, Sakarya University, Serdivan 54050, Turkey
2 Department of Civil Engineering, Faculty of Engineering, Sakarya University, Serdivan 54050, Turkey
* Correspondence: myilmazoglu@kastamonu.edu.tr

Abstract: In general, the ultimate bearing capacity (UBC) of shallow foundations on unsaturated soils is characterized by the conventional shear strength (SS) parameters in which saturated theories are applied. However, in this case, it is clear that the foundations designed using the obtained values from the saturated cases not be economical. In recent years, procedures have been developed to estimate the UBC of foundations on unsaturated soils, that take into account drained and undrained loading conditions. However, these studies generally concentrate on sandy soils. The validity of the results proposed in the literature should be tested for other soils. Therefore, this paper includes a conventional direct shear box (DSB) test to determine the unsaturated SS of statically compacted silty soil, and a series of model tests were performed to determine the foundation's UBC. In the experimental model setup, the UBC values of different types and sizes of model foundations on silty soil layers with a different soil saturation degrees (SSDs)/matric suctions (MSs) and different void ratio values were measured. In addition, the soil-water characteristic curves (SWCCs) and SS parameters of unsaturated silt were obtained. Using the experimental results, a new equation is proposed for the characterization of the UBC of shallow foundations on unsaturated silty soils. Using this equation, the UBC of unsaturated soils can be determined based on the results of unconfined compressive strength tests (UC) measured on unsaturated soil samples and based on the degree of saturation and the fitting parameter. The results indicate that the measured bearing capacity values obtained via the model footing test, shows a good consistency with those obtained by the proposed equation.

Keywords: unsaturated soil; shallow foundation; silt; matric suction; soil–water characteristic curve

Citation: Yilmazoglu, M.U.; Ozocak, A. Bearing Capacity of Shallow Foundations on Unsaturated Silty Soils. *Appl. Sci.* **2023**, *13*, 1308. https://doi.org/10.3390/app13031308

Academic Editors: Xianwei Zhang, Xinyu Liu and Ran An

Received: 28 December 2022
Revised: 13 January 2023
Accepted: 17 January 2023
Published: 18 January 2023

1. Introduction

The design of shallow foundations involves two main objectives: determining the ultimate bearing capacity (UBC) and ensuring compliance with allowable settlement limits. Traditional methods for determining UBC and settlement behavior on saturated soils can be divided into two groups: the Effective Stress Approach [1] (ESA) and the Total Stress Approach [2] (TSA). The ESA requires effective soil parameters and uses c' (effective cohesion) and $\varnothing'$ (effective internal friction angle), whereas the TSA is based on the $\varnothing_u = 0$ analysis and is used for undrained conditions. Until recently, UBC values for footings on unsaturated soil layers were determined based on the assumption of saturated soil [1–3]. However, this assumption is not always accurate and can lead to non-economical solutions. To ensure a realistic design in unsaturated the soil environments, the effect of soil saturation degree (SSD)/matric suction (MS) must be taken into account. MS, which is frequently used as a measure of suction, is a critical characteristic that determines the behavior and mechanical properties of unsaturated soil [4–6]. Therefore, in geotechnical applications, the the MS value must be taken into account when calculating soil strength and volume changes. Capillary tension is the ability of soil to absorb and retain water and is directly related to water content [7].

Research on the behavior of unsaturated soils, which make up a large portion of the Earth's land, has been important in recent years. The majority of shallow foundations are found in areas of unsaturated soil, depending on the depth of the groundwater table. The SS of unsaturated soils is important in the design of shallow foundations because the failure in these foundations is usually caused by exceeding the UBC value [8–11]. Therefore, research on the behavior of unsaturated soils has been prioritized over the last ten years. In the literature, experimental studies have been conducted under both drained and undrained conditions [12–29]. In general, research in this area has aimed to improve understanding of the mechanical behavior of unsaturated soils and to develop appropriate methods for assessing the bearing capacity of unsaturated soils. Studies have focused on factors such as matric suction, soil structure, and soil water content and their effects on the bearing capacity of unsaturated soils. Some studies have also investigated the use of various test methods to assess the bearing capacity of unsaturated soils, such as triaxial tests, direct shear tests, and plate load tests. Additionally, numerical models have been used to simulate the mechanical behavior of unsaturated soils. These studies have shown that the UBC values of foundations, calculated using traditional saturated soil mechanics concepts, are quite far from the UBC values of foundations on unsaturated soil conditions. Studies on the estimation of the UBC of foundations on unsaturated soil layers can be grouped under two main groups, which are similar to traditional soil mechanics groupings. These are the proposed approaches to estimate the SS of unsaturated soils under drained and undrained conditions. There are various structural models and modeling techniques that can be used for both approaches, but these models require a variety of soil parameters that necessitate complex and extensive laboratory tests. On the other hand, there are various numerical modeling techniques presented in the literature that are extended by modifying the ESA and the TSA to take into account the effect of MS [11,12,30–37]. The approaches introduced in the literature are called the Modified Effective Stress Approach (MESA) and the Modified Total Stress Approach (MTSA). These methods, which can be estimated with the test results obtained for unsaturated conditions for the MSEA and the MTSA in the literature, are simple and fast. Additionally, these numerical techniques can be verified by comparing the experimentally measured UBC values with the values obtained through the proposed equations.

Previous studies have shown that the influence of MS on soil strength is not linear [38]. MS is considered to have a non-linear, hydrostatic suction profile. The MS value can change due to changes in the water level or weather conditions, even when the groundwater level is constant [39,40]. This means that foundations on soil layers above the groundwater level may experience larger UBC values than calculations made assuming saturated conditions.

The focus of this research is to use model foundations of various forms and sizes to investigate the UBC of shallow foundations on silty soil. Strength tests and model foundation loading tests on samples with varied void ratios, saturation levels, and the MS values were conducted in order to ascertain the effect of the MS on SS and the UBC values for the unsaturated soil zone.

Estimation of UBC of Foundations on Unsaturated Soils

Several methods have been proposed in the literature for estimating the UBC of foundations on unsaturated soils. These methods mainly involve modifying the equations proposed by Terzaghi [1] and Skempton [2] to take into account the effect of matric suction. Research has shown that foundations on unsaturated soils typically fail through the punching shear failure mode [11,12,15,41]. In the case of cohesive soils, it is assumed the a constant pore water pressure under undrained conditions can provide accurate results. Tang et al. [42] also found that in-place plate bearing tests typically occur under constant water content condition, and that assuming a constant value for the effective stress parameter does not lead to errors in the results. Oh and Vanapalli [18] proposed an equation

(Equation (1)) for estimating the UBC of shallow foundations on the surface of unsaturated fine-grained soil, based on the assumption of an undrained loading condition.

$$q_{ult(unsat)} = s_{unsat} \times \xi \times N_{cs} \tag{1}$$

where $q_{ult(unsat)}$ = UBC of the foundation on fine-grained soil; s_{unsat} = SS of unsaturated soil based on unconfined compressive strength (UC); ξ = shape factor; and N_{cs} = UBC factor under undrained loading conditions (i.e., 5,14). In the same study, Oh and Vanapalli (2013) [18] have also demonstrated that the SS of an unsaturated soil is equal to the sum of the saturated SS and the increase in SS produced by the MS (Equation (2)). In addition, it has been reported that the total SS of the unsaturated cohesive soil (including the contribution of the MS to the SS) can be obtained with the UC, so there is no need to measure the MS value of the cohesive soils [18].

$$s_{unsat} = [s_{sat} + f(u_a - u_w)] = \left[\frac{q_{u(unsat)}}{2}\right] \tag{2}$$

where s_{unsat} is the SS of the soil based on the UC; $f(u_a - u_w)$ is the increase in strength with MS contribution; and $q_{ult(unsat)}$ is the UC of the soil.

Oh and Vanapalli (2013) [18] demonstrated that the UC of fine-grained soils, and mainly of clay soils, can be used to predict the UBC of shallow square foundations (Equation (3)). A shape factor, ξ_{unsat} = 1 + 0.2B/L (where B and L corresponds to the foundation width and length, respectively) established by Meyerhof (1963) [43] and Vesic (1973) [44] for undrained circumstances, was also employed in the proposed equation:

$$q_{ult(unsat)} = \left[\frac{q_{u(unsat)}}{2}\right] \times \left[1 + 0.2\frac{B}{L}\right] \times N_{unsat} \tag{3}$$

where B is the width of the foundation; L is the length of the foundation; and N_{unsat} is the UBC factor in unsaturated soils, which was obtained using back analysis by Oh and Vanapalli (2013) [18].

In addition, for the estimation of the UBC of foundations on coarse-grained unsaturated soils under drained loading conditions, equations based on the modification of the UBC equation (Equation (4)) proposed by Terzaghi (1943) [1] for strip foundations on saturated soils is available in the literature [12,13,15,26,29,30,32,34].

$$q_{ult} = K_1 c' N_c + q N_q + K_2 \gamma B N_\gamma \tag{4}$$

where c' is the effective cohesion; q is the effective vertical stress; B is the width of foundation; K_1 and K_2 are shape factors; and N_c, N_q and N_γ are UBC factors.

Oloo et al. (1997) [12] modified Terzaghi's (1943) [1] effective stress approach and proposed a model that can be used to estimate the UBC of a shallow foundation on unsaturated soils, taking into account the effect of MS (Equation (5)). The model covers the situation in which both pore air and water pressure are effective during the loading phase. The model employs a fixed $\varnothing^b$ for suction values greater than the air-entry value (AEV) of the soil.

$$q_{ult} = \left\{c' + (u_a - u_w)_b tan\varnothing' + [(u_a - u_w) - (u_a - u_w)_b]tan\varnothing^b\right\}N_c + \frac{1}{2}B\gamma N_\gamma \tag{5}$$

where c' is the effective cohesion; $\varnothing'$ is the effective angle of internal friction; $\varnothing^b$ is the angle indicating the rate of increase in shear strength relative to the MS; $(u_a - u_w)_b$ is the AEV/bubbling pressure; $(u_a - u_w)$ is the MS value; B is the width of the foundation; N_c and N_γ are the UBC coefficients of Terzaghi (1943) [1] and Kumbhokjar (1993) [45], respectively. Since the behavior of $\varnothing^b$ is non-linear beyond the AEV, this method can estimate the UBC within an acceptable range depending on the suction range. A bilinear envelope [46] can be used to simulate the nonlinear relationship between the SS and the MS, as shown in

Figure 1. As can be seen from Figure 1, the contribution of MS to the SS is $\varnothing^b = \varnothing'$ for suction values less than the AEV. This region, where the SS increases linearly with the MS, is called the linear region. Beyond the AEV, the contribution of $\varnothing^b$ gradually decreases despite the increase in MS; therefore, $\varnothing^b$ is less than $\varnothing'$. In this region, which is called the nonlinear region, the SS of unsaturated soils changes nonlinearly with the MS [46,47]. Such a behavior is consistent with the reason explained using Figure 1 for the SS of unsaturated soils. The red line here shows the contribution of $\varnothing^b$, to the SS at MS values greater than the AEV.

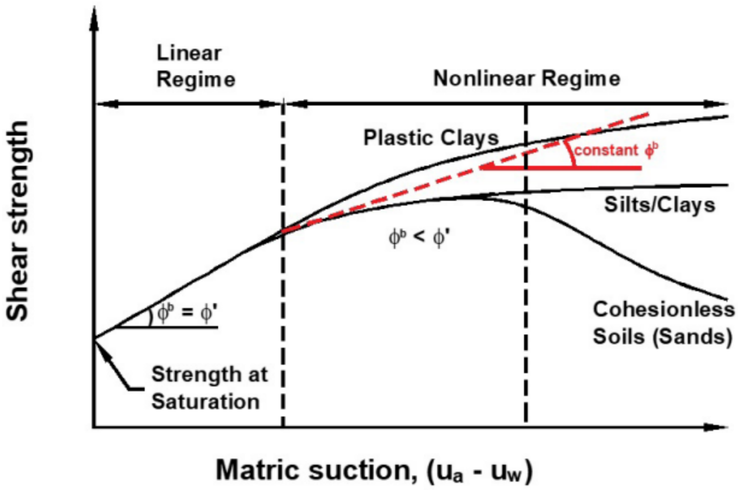

Figure 1. The effect of MS value on SS [46].

Vanapalli and Mohamed (2007) [14] developed the original UBC equation for continuous footings which was based on the Terzaghi (1943) [1] equation for unsaturated soils and reference the UBC model of Oloo et al. (1997) [12], and the nonlinear shearing resistance model proposed by Vanapalli et al. (1996) [48] (Equation (6)). Vanapalli and Mohamed (2007) [14] also suggested that by using the measured shear strength angle value increased by 10% (1.1ϕ′), a more accurate estimation of the UBC value can be obtained for both saturated and unsaturated conditions.

$$q_{ult} = \left\{ \left[c' + (u_a - u_w)_b tan\varnothing' - S^{\Psi} tan\varnothing' \right] + (u_a - u_w)_{AVE} S^{\Psi} tan\varnothing' \right\} N_c \xi_c + \frac{1}{2} B \gamma N_\gamma \xi_\gamma \tag{6}$$

where c' is the effective cohesion; $\varnothing'$ is the effective angle of internal friction; S is the degree of saturation; Ψ is the fitting parameter; $(u_a - u_w)_b$ is the AEV; $(u_a - u_w)_{AVE}$ is the average MS value; N_c and N_γ = are Terzaghi (1943) [1] and Kumbhokjar (1993) [45] bearing capacity coefficients, respectively, and ξ_c and ξ_γ = Vesic (1973) [44] shape factors.

Vanapalli and Mohamed (2007) [14] developed a correlation between the UBC fitting parameter (Ψ) and the plasticity index (I_p) based on the results of the study performed on five soils (Figure 2). All three of the sandy soils examined in the study had a fitting parameter (Ψ) = 1; however, it was noted that other fine-grained soils needed greater values. Equation 7 explains the link between the UBC fitting parameter (Ψ) and the I_p based on the findings of the research conducted on five soils.

$$\Psi = -0.0031 I_p^2 + 0.34 I_p + 1 \tag{7}$$

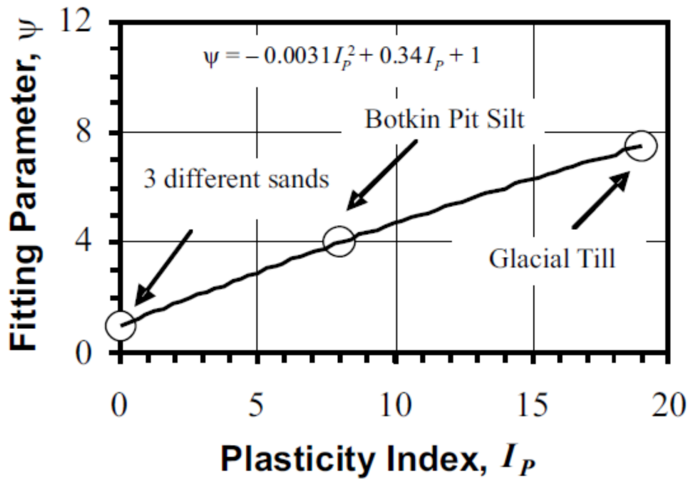

Figure 2. The relationship between Ψ and I_p [14].

In this study, a new equation is proposed in which the UBC of foundations on unsaturated silty soils is determined by adopting the total stress analysis philosophy presented above, with a bearing capacity fitting parameter (S^{Ψ}) based on the SS determined via the UCS tests and the SSD/MS value.

Various models have been proposed in the literature to estimate the UBC of unsaturated soils (see Table 1). Some of these proposed equations directly use the MS value, whereas the other group indirectly uses MS.

Table 1. Bearing capacity models for unsaturated soil.

Authors	UBC Equation	Soil Type
Oloo et al. (1997) [12]	$q_{ult} = \left\{c' + (u_a - u_w)_b tan\varnothing' + [(u_a - u_w) - (u_a - u_w)_b]tan\varnothing^b\right\}N_c + \frac{1}{2}B\gamma N_\gamma$	-
Vanapalli & Mohamed (2007) [14]	$q_{ult} = \{[c' + (u_a - u_w)_b tan\varnothing' - S^{\Psi} tan\varnothing'] + (u_a - u_w)_{AVE} S^{\Psi} tan\varnothing'\}N_c\xi_c + \frac{1}{2}B\gamma N_\gamma \xi_\gamma$	Poorly graded sand
Oh & Vanapalli (2013) [18]	$q_{ult(unsat)} = \left[\frac{q_{u(unsat)}}{2}\right] \times \left[1 + 0.2\frac{B}{L}\right] \times N_{unsat}$	Low plasticity clay
Vahedifard & Robinson (2016) [32]	$S_e = \left(\frac{1}{1+\left\{-ln\left(1+\frac{q}{k_s}\right)e^{-\gamma_w \alpha z} - \frac{q}{k_s}\right\}^n}\right)^{n-1/n}$	-
Tang et al. (2017) [42]	$q_{ult} = [c' + (\chi^s)_{AVE} tan\varnothing']N_c d_c + q_{ult} q N_q d_q + 0.5\gamma B N_\gamma d_\gamma$	-
Garakani et al. (2020) [37]	$q_{ult} = [c' + c_{AVE}]N_c\xi_c + qN_q\xi_q + 0.5B\gamma N_\gamma + s(N_s)_{cst} tan\varnothing^b \xi_s$	Poorly graded sand
Zhang et al. (2020) [17]	$q_{ult} = \left[c' + (u_a - u_w)_m tan\varnothing^b\right]N_c^M + \sigma_0 N_q^M \frac{1}{2}(B\gamma - u_a)N_\gamma N_\gamma^M$	Sand

2. Materials and Methods

2.1. Material

Soil samples taken from the city of Adapazarı were used in the experimental studies to examine the change in the UBC of the shallow footings on unsaturated soils. The samples were taken from the Yenigün District of Adapazarı (Turkey), at a depth of 3–4 m. The properties of the silty soil sample used in this study according to ASTM D4318 [49] are given in Table 2. The soil sample was classified as low plasticity silt (ML) according to the USCS. Figure 3 shows the grain size distribution curve of the sample.

Table 2. Physical properties of the soil used in the experimental study.

Property	Value	Symbol and Unit
No 200#	89	FC (%)
Liquid limit	35.8	LL (%)
Plastic limit	25.2	PL (%)
Plasticity index	10.6	IP (%)
Specific gravity	2.692	G_s
Clay ratio	17	C (%)
Silt ratio	72	M (%)
Sand ratio	11	S (%)
Soil class: Low Plasticity Silt (ML)		

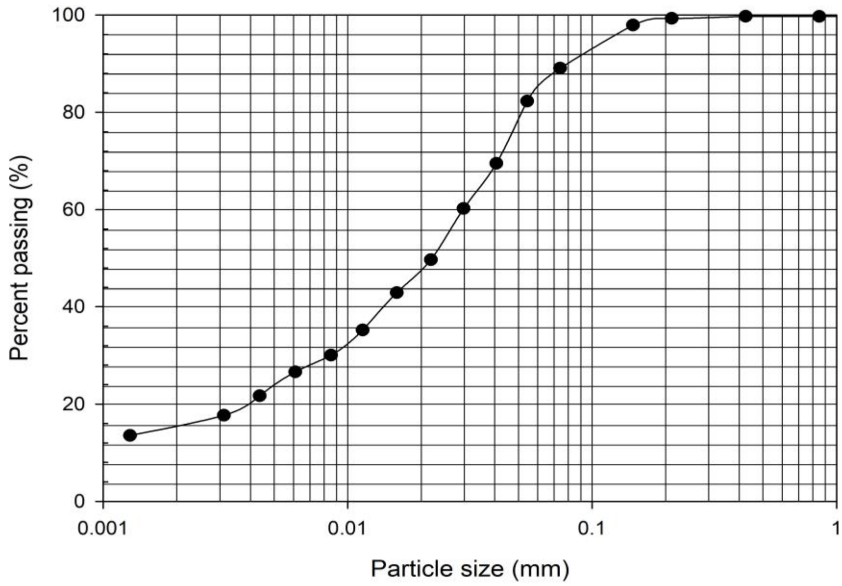

Figure 3. Grain-size distribution of samples used in the study.

The mineralogical composition of the silt used in this study was determined with an X-ray diffraction analysis and is shown in Table 3. It indicates that elements such as calcium oxide and magnesium oxide, which are the primary cementing agents in the soil, are present in significant amounts in the soil sample [50,51]. However, studies in the literature have demonstrated that the cementing bonds that are disrupted in remolded samples do not re-form [50,52]. As a result, when compared to experiments carried out on in situ or undisturbed materials, the cohesiveness of the remolded samples is lower. Furthermore, research suggests that the shear resistance angle is less influenced than the cohesion value [53].

Table 3. Mineralogical properties of the soil sample.

Symbol	Element	Value (%)
SiO_2	Silicon dioxide	40.94
Al_2O_3	Alumina	11.09
Fe_2O_3	Iron oxide	5.36
MgO	Magnesium oxide	4.48
CaO	Quicklime	15.58
K_2O	Potassium oxide	1.72
Na_2O	Sodium oxide	2.09
TiO_2	Titanium oxide	0.82
-	Other	17.92

2.2. Method

In this study, the ultimate bearing capacity (UBC) of shallow foundations on unsaturated soils was investigated. The basic physical properties of silt samples taken from Adapazarı were determined and void ratios were selected for use in experiments. The natural void ratios of silts in Adapazarı were examined [54], and samples with void ratios of 0.65, 0.70, and 0.75 were used in the experiments. The sample SSDs were set at 65%, 70%, 75%, and 85% to account for seasonal groundwater level changes in Adapazarı. The shear strength angle and cohesion values of the silt samples were obtained by using direct shear tests.

The SS parameters of unsaturated soils can be measured using a modified MS-controlled triaxial apparatus or a direct shear box (DSB) test [53,55–57]. However, these methods can be costly and time-consuming, and the results are not as practical as those from the saturated state. A more widely accepted method is to combine the application of the targeted suction magnitude with a DSB test. Studies have shown that this method is consistent with the results obtained using a modified DSB test capable of MS control [53,58–60]. In this study, the shear strength of unsaturated Adapazarı silt was determined using a conventional direct shear test. The samples were prepared at the targeted SSD, and MS values were measured using a pressure plate and filter paper. The shear box test was carried out on a fully automatic direct shearing apparatus with a square shear box 6 × 6 cm in diameter and 2.5 cm in height. During the test, the samples were carefully isolated from air to maintain their saturation degree/suction values. The $\varnothing^b$ values of silt soil were calculated from the test results and MS values, and the UBC was determined using these values.

The relationship between the WC/SSD and MS is important in evaluating the behavior of unsaturated soils. In this study, the MS values of the samples were determined using the filter paper method and pressure plate method to create the SWCCs. The filter paper method, which was proposed in the 1930s, is an economical but slow method for measuring suction, and it can measure total and the MS values up to 30 MPa [61]. This method uses a filter paper whose calibration curve is known and places it in full contact with the sample to determine pore water flow. The measurement period is 6–8 days. After the moisture balance is achieved, the wet and dry weight of the filter paper is weighed on a balance with a sensitivity of 0.0001 g, and the corresponding MS value is found in the calibration curve according to the filter paper water content. The SWCC of the sample is formed by repeating these processes at different WCs from the saturated state to the air-dried state [28,62]. In this study, the MS values were determined with the filter paper method by using the calibration curve recommended for the Whatman No. 42 filter paper in ASTM 5298-92 [63].

The pressure plate method is used to apply suction using the axis translation technique [64]. Air pressure (u_a) is applied to the samples placed on a ceramic with the high AEV in the steel cell coming from the inlet at the top of the cell, and pore water pressure (u_w) is applied trough the inlet connected to the ceramic. This process must be continued until the water flow is balanced [28,65]. When the water at the output reaches equilibrium after the applied suction, the sample weight/volume is taken and the next suction stage is started. The MS (u_a–u_w) values were applied in incremental steps from 5 kPa to 1500 kPa. A 1500F1 pressure plate extractor with a 15-bar capacity was used to conduct the pressure plate experiments.

The UBC of foundations on unsaturated silt soils was examined by model tests. Previous research and experimental studies have shown that the applied loads will have no effect on the boundaries of the sample container if the soil model tank size is 6 or more times higher than the model foundation size [14,66,67]. For this reason, of the soil tank used in the current study was chosen to be greater than 6 times higher than the model foundation dimensions. The model test used a cylindrical model test box with a height of 240 mm and a diameter of 310 mm filled with the soil sample at the desired void ratio and soil saturation degree values. The foundation bearing capacity was investigated with the help of 50 mm diameter circle, 50 × 50 mm square, 42.3 mm circle, and 37.5 × 37.5 square foundation models placed on the model test box. The 42.3 mm circle and 37.5 × 37.5 mm square foundations were selected for further experiments as they have an equal base area.

Sample Preparation

The silty soil taken from the Adapazarı city center was first air-dried in the laboratory environment. The air-dried sample was pulverized by hand. In order to prepare the samples homogeneously at the desired water content, it was sieved through the No.10 (2 mm) sieve with for the maximum grain diameter, both to prevent lumping and to remove organic substances. The sieved soil sample was divided into groups of 2 kg, which were wetted by spraying deionized and deaired water for the desired degree of saturation was reached and mixed with the help of a sample preparation mixer. This process was repeated for each sample of different VR and SSD values. The prepared soil samples were placed in airtight containers and left at room temperature for 24 h for curing. With this procedure, a homogeneous soil-water mixture was obtained with no measurable difference between the desired WCs. After the standard 24 h curing period was completed, three different samples were taken from the different parts of each airtight container to check the WC and it was confirmed that the WCs of the mixtures in all the bags were equal within a ±0.5% evaporation/moisture change margin of error.

The prepared soil samples were compacted at a statically constant velocity in a model tank specifically designed for hydraulic press equipment. A metal plate with a diameter of 305 mm and a thickness of 30 mm was used as the clamping apparatus. While preparing the samples for the model experiments, they were statically compacted into two layers to obtain a homogeneous void ratio. By creating scratches between the layers, adherence losses that could occur between these layers were prevented. For each VR and SSD values, a prepared and cured soil sample equal to the calculated sample weights by using the volume-weight ratio of the soil was statically compacted in the model tank. After the UBC tests were carried out, two specimens were taken out from the compacted sample using 50 mm diameter stainless steel thin-wall tubes for the UC test. With the help of a small cylindrical sample mold that had a certain volume which was obtained from the model test mold, the weight and the WC measurements of the samples taken from different depths, as well as the VR and SSD were checked. In addition, the MS values were measured using the filter paper method on samples with a height of 20 mm and a diameter of 50 mm, which were taken from depths of 0.5B and 1.5B (Figure 4).

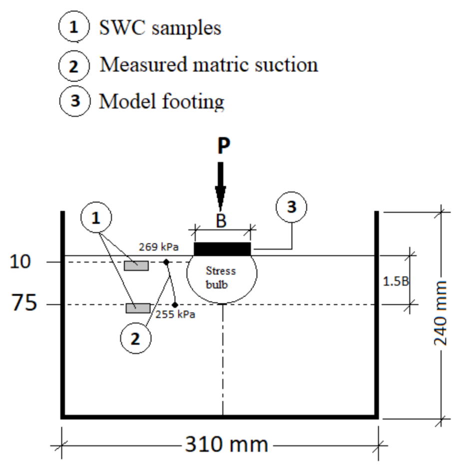

Figure 4. Schema showing the procedure used to determine the MC under the foundation.

The samples for the DSB test were statically compacted, the same as those used in the model footing testing. The samples, prepared with the WC values corresponding to the desired MS values from the SWCC curves, were insulated from the air with silicone grease so that there was no loss in the WC during rapid shearing and no change in the MS value [53,58,68]. The shear rate applied in this study was determined to be 1.15 mm/min after considering other studies in the literature [12,14,53,60]. Experiments on the model load tests were run as displacement-controlled tests. According to earlier research on compacted samples, soil specimens can reach drained conditions when loaded at a strain rate between 0.0102 mm/min and 0.0132 mm/min [46,48]. In the current investigation, undrained loading conditions were simulated using a reasonably quick loading rate of 1.15 mm/min. The DSB tests were conducted in accordance with the ASTM D3080-98 [69] at normal stress levels of 59, 98, and 147 kPa. Due to the fast loading rate applied in the direct shear tests, the undrained shearing conditions were assumed to prevail. In order to confirm the assumption that there is no change in the gravimetric water content (GWC) value of the samples during the DSB test process, the sheared samples were subjected to MS and WC measurements directly after the test.

3. Results and Discussion

After the soil samples were created for the pressure plate tests and filter paper tests, they were statically compressed, as was carried out for the other tests, and the samples were taken with the help of metal rings with a diameter of 50 mm and a height of 20 mm. The samples were fixed by placing porous stones on the samples in order to reach the SSD and were kept in distilled water for 7 days. The samples taken from the model loading tests, on the other hand, were placed immediately on the filter paper to start the equilibrium stage and the MS values of the prepared samples were measured.

The SWCCs of the samples formed at three different void ratios were determined by the pressure plate and filter paper method. In the experimental study, model tests were conducted with soil samples compacted with targeted VRs (0.65, 0.7 and 0.75) and SSDs (i.e., 65%, 70%, 75%, 85%, 100%) considering seasonal groundwater level changes. To reflect this scenario, the samples were statically compressed with targeted VRs at four different SSDs. Since experiments were carried out on samples with three different VRs, the samples were prepared at these VRs for the SWCC experiments. Therefore, SWCC experiments were carried out on three samples (0.65, 0.7 and 0.75 void ratios) and SWCCs have been created according to the GWC. The most ideal curves of the experimental data were created with the Van Genuchten (1980) [70] model, which is one of the SWCC generation models available in the literature, for MS values ranges between 0 and 1,000,000 kPa (Figure 5). Since the SWCC data at high MS range could not be determined with the pressure plate (the suction was determined with the pressure plate up to 800 kPa), it was measured by the filter paper method, and it was again found to be compatible with the curves obtained from the Van Genuchten (1980) [70] model. The AEVs of the samples with 0.65, 0.70 and 0.75 void ratios have been determined as 12.4, 10.2 and 8.0 kPa, respectively.

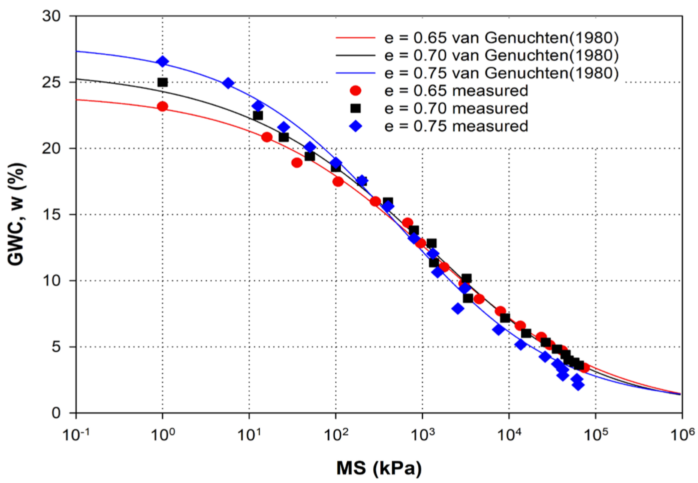

Figure 5. SWCCs of silty soil prepared at different VRs.

Samples with VRs of 0.65, 0.70 and 0.75 and SSDs of 65%, 70%, 75%, 85% and 100% were created using static compression. The samples were saturated under water for 9 days. The SS were recorded as a function of horizontal displacement up to the maximum value. As seen in Figure 6, a clear peak is observed in the stress-strain graphs at each net stress (59, 98 and 147 kPa) at MS values higher than the AEV in the samples with 0.65 VR. No significant peak has been observed for the saturated state. A similar situation is observed for the samples with VRs of 0.70 and 0.75.

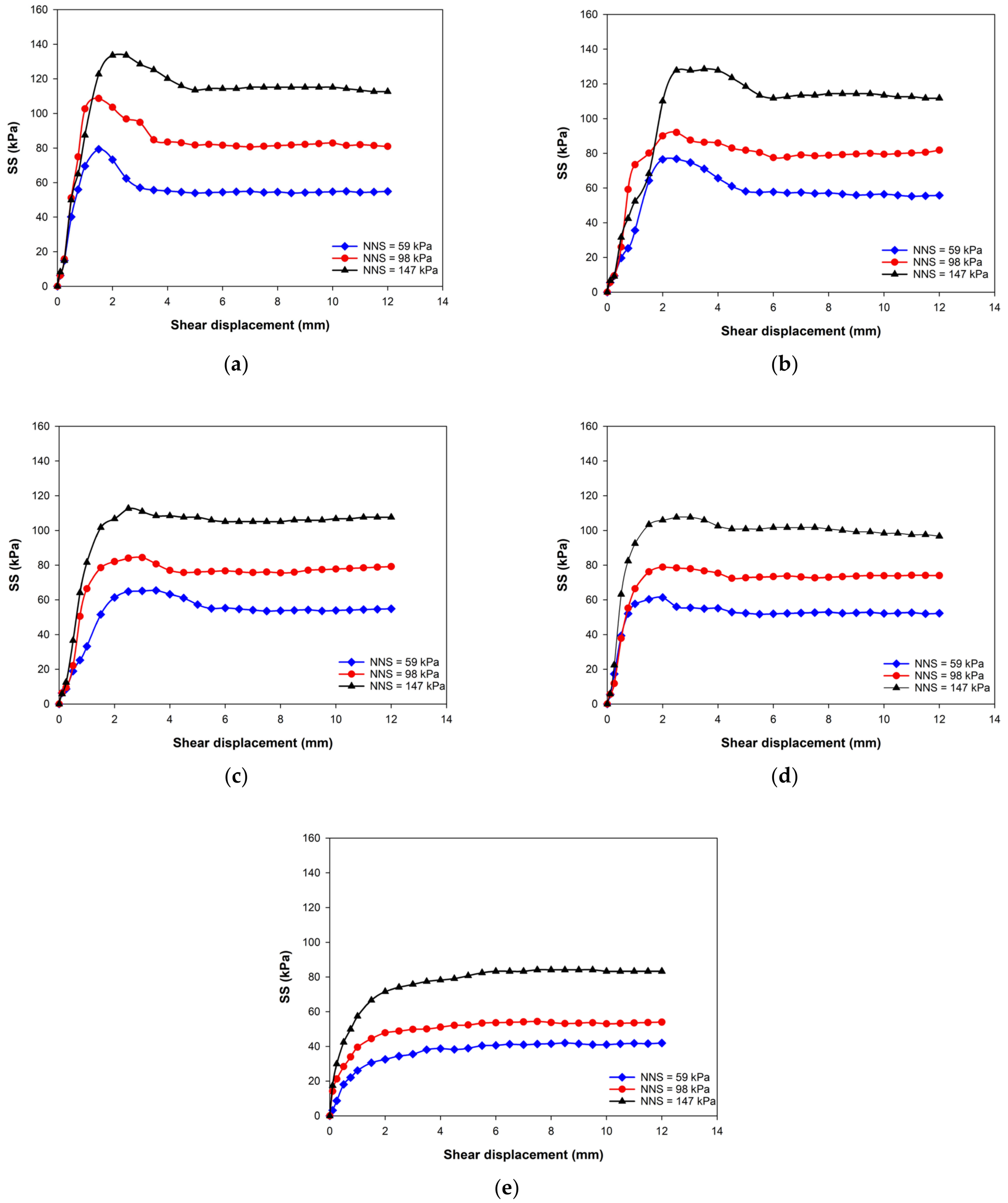

Figure 6. Shear strain curves for silt sample with VR = 0.65 (from shear box tests): (**a**) SSD = 65%; (**b**) SSD = 70%; (**c**) SSD = 75%; (**d**) SSD = 85%; (**e**) SSD = 100%.

In each VR, the MS values taken from the SWCCs and the results of the shear box test performed at 65%, 70%, 75%, 85% and 100% saturation degrees were combined, and the MS—SS net normal stress (NNS) plots were drawn (Figure 7). The $\varnothing^b$ values calculated on these graphs are presented in Table 4. When Table 4 is examined, it is seen that lower $\varnothing^b$ values are calculated for the three different VRs at low NNS. The increase in the VR also increases the $\varnothing^b$ value.

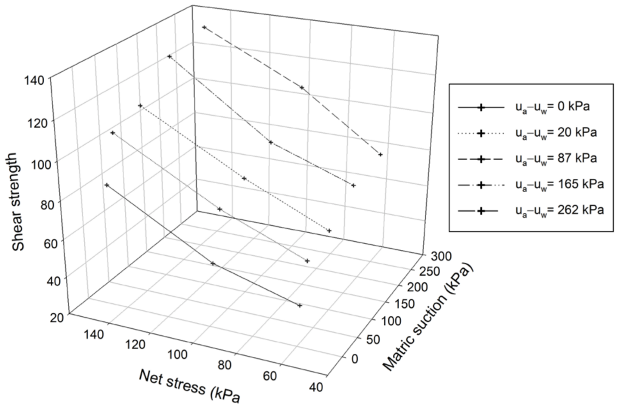

(**a**)

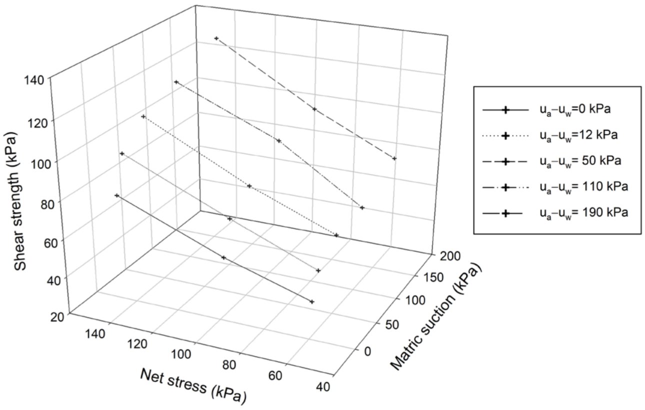

(**b**)

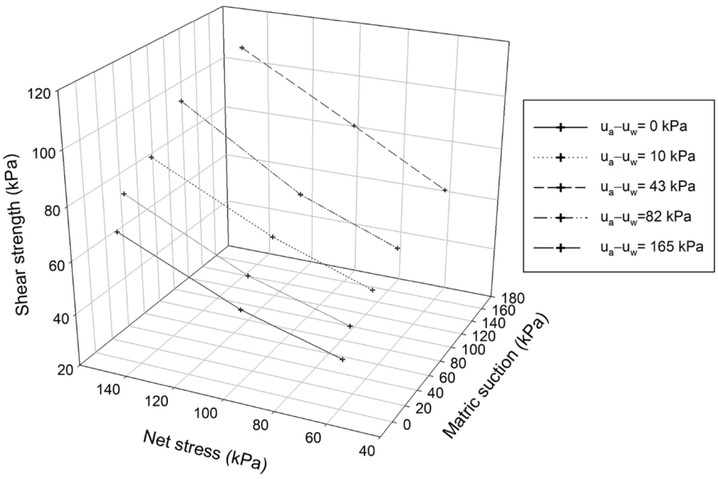

(**c**)

Figure 7. MS-NNS-SS variation for void ratios: (**a**) VR = 0.65; (**b**) VR = 0.70; (**c**) VR = 0.75.

Table 4. Angles showing the slope of the SS increase with respect to the MS.

e	$(\sigma_n - u_a)$ kPa	$\varnothing^b$	$\varnothing^b_{average}$
0.65	59 98 147	4.6 7.6 7.2	6.5
0.70	59 98 147	5.7 7.1 9.0	7.3
0.75	59 98 147	5.6 8.8 10.0	8.1

Figure 8 shows the failure envelopes formed by considering the maximum SS values of the samples. Table 5 lists the SS parameters of the soils obtained from these failure envelopes. With the increase of the SSD, a decreasing trend is observed in the cohesion values and the SS angles of the samples with three different VRs. In the literature, it is a known behavior that a decrease in the SSD/increase in the MS value will cause an increase in the cohesion value [55]. In addition, the observation that the increase in the MS value causes an increase in the angle of SS is compatible with the data of Wen and Yan (2014) [53].

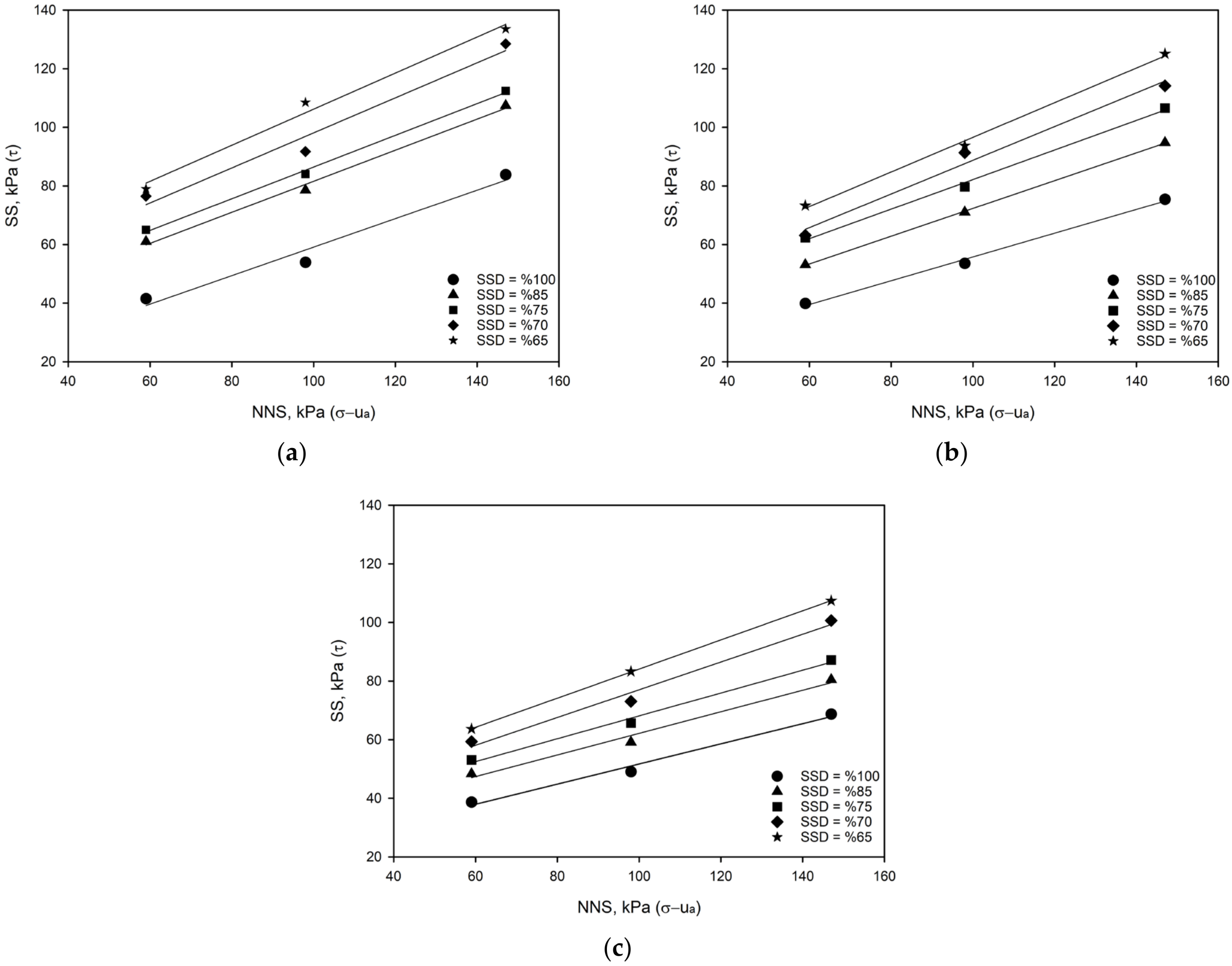

Figure 8. SS-SSD relations under different VR and NNS: (**a**) VR = 0.65; (**b**) VR = 0.70; (**c**) VR = 0.75.

Table 5. SS parameters of samples with different SSD.

e	SS Parameters	SSD, %				
		100	**85**	**75**	**70**	**65**
0.65	c	5.5	29.1	32.9	38.8	45.1
	∅	27.4	27.8	28.3	30.8	31.5
0.70	c	7.1	31.7	39.1	38.9	45.9
	∅	24.2	22.6	23.8	26.9	27.6
0.75	c	9.6	30.9	35.1	36.8	41.5
	∅	21.1	17.8	18.8	22.4	23.5

Figure 9 shows how the SS of silt soils tested at three different VRs varies with both the NNS and the SSD. The results show that the effect of the SSD on the SS decreases as the NNS value increases. In the tests carried out under NNSs of 59 and 98 kPa, there was a peak/trough fluctuation between the SSDs of 70% and 75% SSDs. This shows that in addition to the MS of the silty soil sample, a different void structure has the strongest or weakest effect on the SS at a certain SSD [53,60].

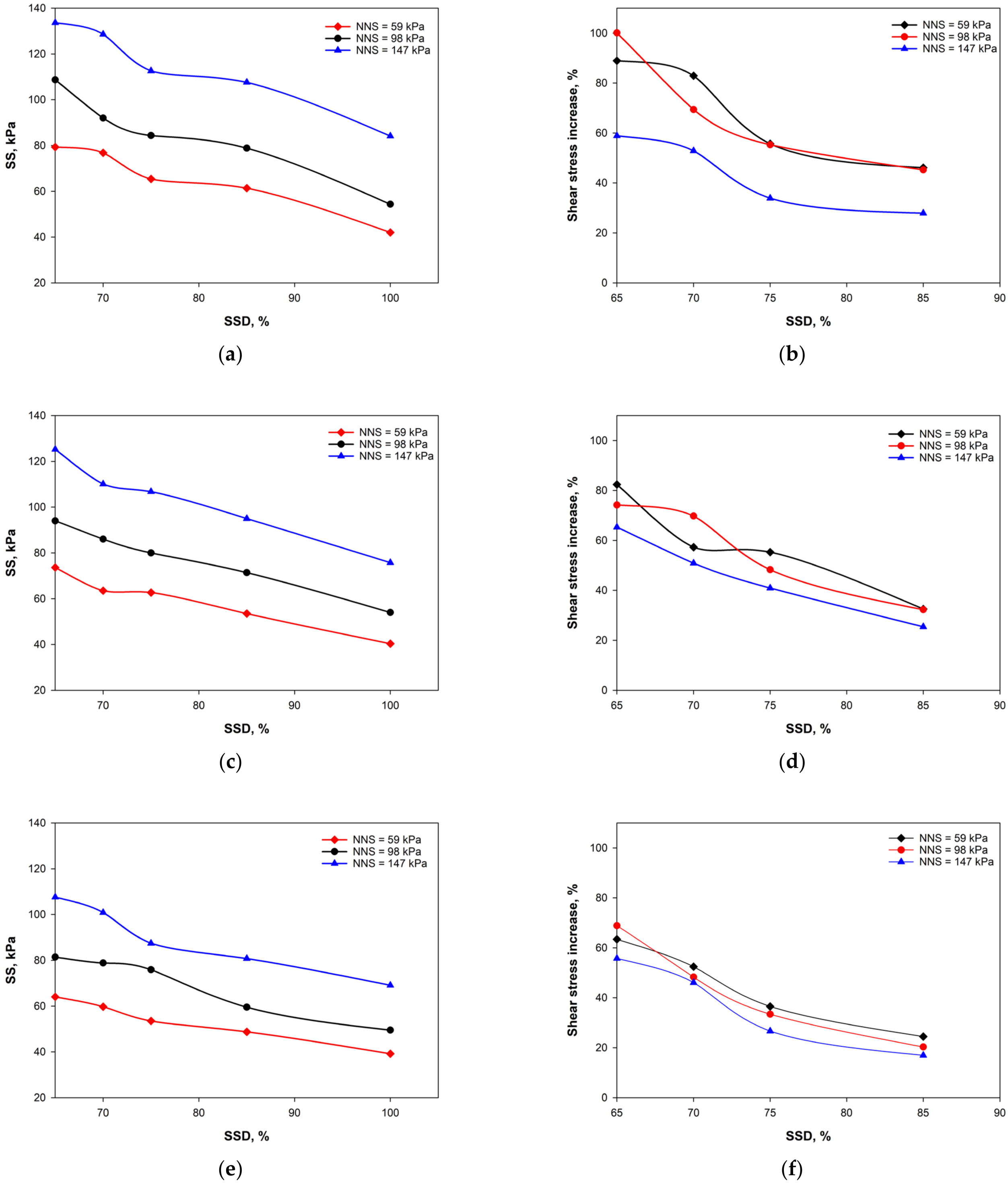

Figure 9. Saturation-shear stress relationships: (**a**) VR = 0.65; (**c**) VR = 0.70; (**e**) VR = 0.75, Saturation-% shear stress increase relationships: (**b**) VR = 0.65; (**d**) VR = 0.70; (**f**) VR = 0.75.

In the current work, model foundations experiments were conducted in a cylindrical tank filled with statically compacted soils to examine the UBC of foundations on unsaturated soils under undrained loading circumstances. The model foundations were loaded relatively quickly (1.15 mm/min) to avoid any changes to the suction value of the sample during the loading process. Square and circular shallow foundation models were loaded up to the peak failure conditions to determine the UBC. The dimensions of the glass fiber reinforced polyester tank used are 310 mm in diameter, height of 250 mm and a thickness of 10.2 mm. Model foundations with the largest foundation width of 50 mm were employed in the study. The dimensions of the model mold were selected large enough (>6D) that stresses on the boundaries of the mold due to the loads applied to the model foundation would have a negligible effect. It was confirmed by the control measurements carried out during the tests that no deformation occurred in the mold (The deformation was checked at three different measurement points on the outer surface of the mold.) during loading. Model foundation loadings were performed by using a triaxial loading frame. The vertical displacements of the model foundations were measured with the deformation gauges, and the loads were measured using a load cell (Figure 10). In both measurements, the data were recorded by taking their values at the predetermined deformations. Tests were terminated until the settlements reached 20 percent of the foundation width.

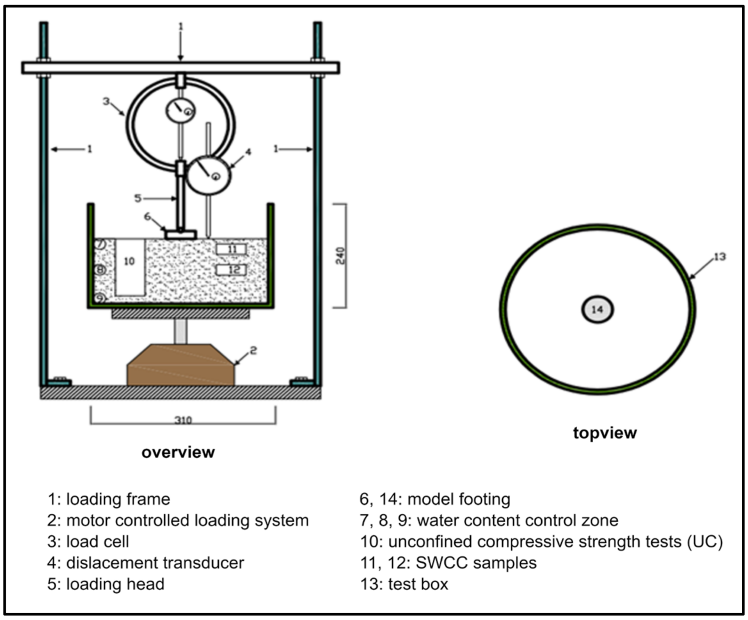

(**a**)

(**b**)

Figure 10. Model test setup: (**a**) schematic; (**b**) experimental picture.

After the UBC tests were performed, two samples were taken from the compacted soils using 50 mm diameter stainless steel thin-walled pipes. A total of 96 UC test were performed on the samples taken. The average values of 12 different scenarios when classified with similar VRs and SSDs are shown in Table 6.

Table 6. Angles showing the slope of the SS increase with respect to the MS.

SSD, %	VR = 0.65	VR = 0.70	VR = 0.75
	q_u (kPa)	q_u (kPa)	q_u (kPa)
65	116.05	71.88	54.31
70	94.68	65.19	37.99
75	75.58	58.89	31.23
85	68.2	36.57	29.31

The model footing test results for both saturated and unsaturated silt sample prepared at the VR of 0.65 are shown in Figure 11. As seen, no clear failure point has been observed in the curves. Therefore, the UBC values have been evaluated by intersecting the tangents of the initial and the final linear part of the curves.

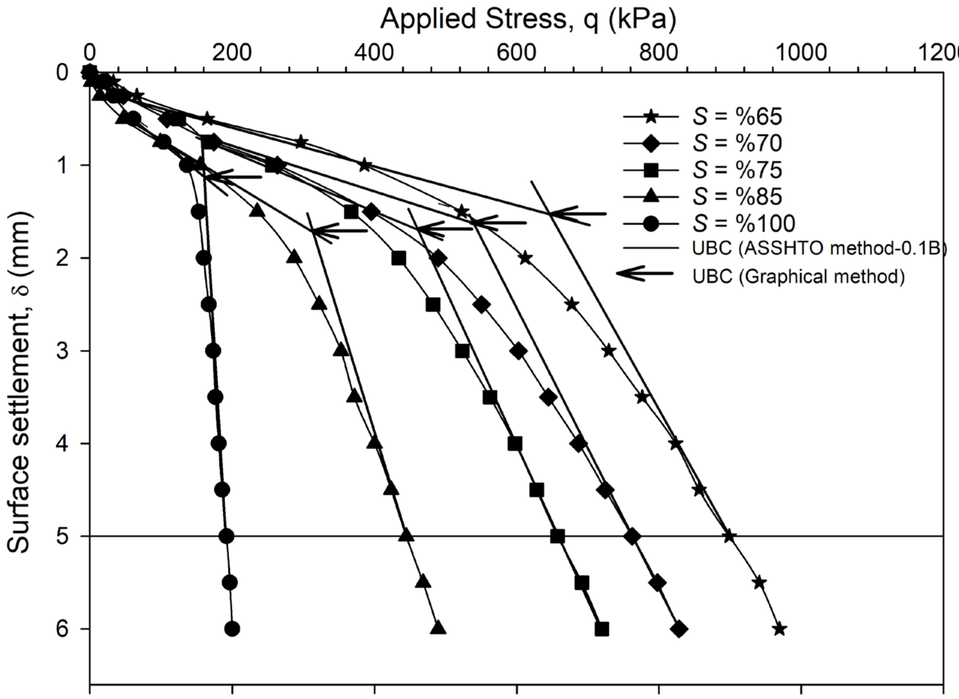

Figure 11. UBC model test results (VR = 0.65 and 50 mm circular model foundation).

The state of the soil and punching shear failure after the model footing tests can be observed from Figure 12. In the punching failure described by Vesic (1973) [44], which is also valid in the current study:

1. A peak is not observed,
2. Except for where the load is applied, no soil heave is visible, and
3. It is defined that it is created by the vertical shear and compression of the soil immediately beneath the footing.

(**a**) (**b**)

Figure 12. Soil settlement after loading test and cracks around model foundation: (**a**) 50 mm × 50 mm square; (**b**) 50 mm circle.

In such cases where the peak is not observed, the UBC of the foundation (q_{ult}) is determined in accordance with ASTM (D1194) [71]. The UBC is defined by ASTM (D1194) [71] as a stress value equal to one tenth (0.1B) of the foundation width. In addition, Steensen-Bach et al. (1987) [72] and Costa et al. (2003) [13] graphically determined the UBC by expanding the elastic and plastic parts of the loading curves profile. In Figure 11, the UBC values were calculated via both the graphical method (with the intersection point of the two linear sections) and the stress value corresponding to the 0.1B settlement value. With the use of the method valid in the literature, the UBC values corresponding to 0.1B have been taken into account in the next evaluations.

In this study, a total stress-based approach was employed. The most crucial part of the paper is introducing a new relationship that can estimate the UBC of foundations on unsaturated silty soils from the UC test and also estimate the UBC fitting parameter (S^{Ψ}) depending on the soil saturation (Equation (8)).

$$q_{ult(unsat)} = \left[\frac{q_{u(unsat)}}{2}\right] \times \left[1 + 0.2\frac{B}{L}\right] \times N_{cs} \times S^{\Psi} \quad (8)$$

where $q_{ult(unsat)}$ is the UBC of the foundation on silty soil; $q_{u(unsat)}$ is the SS of unsaturated soil-based on UC; B is the width of the foundation; L is the length of the foundation; N_{cs} is the UBC; S is the degree of saturation; and Ψ is fitting parameter.

At the end of the experimental studies, the model tests performed on silty soil (72% silt content) showed that the UBC of the foundations was different from that of the foundations on sand or clay soils studied in the literature. As it is known, the behavior of silts is neither exactly similar to clays nor sands, and nor is it the average of the reactions of two neighboring soil types. Silt soils are not under fully undrained conditions as clay soils are, nor are they under drained conditions as sandy soils are. Therefore, a critical part of the unsaturated soil mechanics must be studied to better understand the characterization of the unsaturated silty soils. The results obtained were also plugged into the equations proposed by Oloo et al. (1997) [12] and Vanapalli and Muhammed (2007) [14] for the estimation of a foundation's UBC of unsaturated soils and the results were compared.

Table 7 summarizes the measured the UBC values for all model foundations, including those estimated using the MTSA (i.e., Equations (3) and (8)), and those estimated using MESA (i.e., Equations (5) and (6)). The mean S^{Ψ} values, which were back calculated by using the Equation (8) suggested in this paper, have been found to be −2.89 and −1.33 when the UBC values were determined using 0.1B settlement and graphical methods, respectively. As can be seen from Table 6, although the difference between the calculated UBC values and the measured UBC values is small, the difference between the measured UBC values and the UBC values calculated with Equation (3) [i.e., that estimated using the value $N_{c(unsat)}$ = 5.14 as suggested by Oh and Vanapalli (2013) [18] and the modifications of Skempton (1948) [2] is large.

Equation (6), which is one of the models that estimate the UBC using the MESA, estimated very high UBC values compared to both the graphical method and the UBC values corresponding to the 0.1B settlement. However, Equation (5), which calculates the UBC by using the SS parameters, $\varnothing^b$ values, and MS values, gives reliable results for the MS values equivalent to an SSD of 85%, 75% and 70%, according to the UBC values calculated with 0.1B method. In cases where the MS value is high, the model gives very high values according to the test results. The main reason for this is that the model proposed by Oloo et al. (1997) [12] takes into account the increase in SS after high MS values are reached and as the residual WC approaches saturation. It is seen that there are great differences between the UBC values estimated via Equation (5) and the UBC values calculated by using the graphical method on the model test data. In addition, there are significant differences between the UBC results obtained with the test data (and proposed with Equation (8)) and the method produced by Oloo et al., (1997) [12].

Table 7. Model test results and estimated bearing capacity values.

Model Footing	VR	SSD %	WC %	MS kPa	Oloo et al., 1997 (Equation (5))	Vanapalli & Muhammed 2007 (Equation (6))	Oh & Vanapalli 2013 (Equation (3))	0.1B Settlement Method (Exp)	Grap. Method (Exp.)	UBC (Equation (8))	Ψ 0.1B Method	Ψ Grap. Method
50 mm Circle	0.651	64.2	15.69	284.1	1300	1501	348	899	648	826	−2.89	−1.33
	0.647	70.1	16.90	165.96	939	1318	292	762	550	597		
	0.648	74.4	18.00	91.90	712	1121	233	658	470	415		
	0.656	83.8	20.41	21.54	497	767	210	445	300	291		
	0.696	64.3	16.70	229.09	983	934	222	588	385	526	−2.89	−1.33
	0.699	68.6	17.80	141.25	752	857	201	499	345	411		
	0.701	74.5	19.40	63.10	547	679	182	372	280	323		
	0.702	83.2	21.70	15.61	423	521	113	213	140	156		
	0.749	64.7	17.99	157.28	645	587	167	424	320	397	−2.89	−1.33
	0.75	70.5	19.67	82.54	484	522	117	346	210	240		
	0.756	75.5	21.19	28.18	367	426	96	255	180	171		
	0.75	84.4	23.51	14.02	336	413	90	187	110	125		
50 mm × 50 mm Square	0.652	64.8	15.70	284.01	1294	1255	348	905	625	826	−2.89	−1.33
	0.650	69.4	16.80	174.16	958	1136	292	773	560	597		
	0.655	73.9	18.00	91.90	706	946	233	595	410	415		
	0.647	84.1	20.22	23.99	498	567	210	425	290	291		
	0.699	63.7	16.60	241.73	1016	890	222	548	375	526	−2.89	−1.33
	0.701	68.4	17.80	141.25	752	812	201	503	355	411		
	0.706	75.2	19.70	56.67	531	663	182	360	250	323		
	0.706	83.6	21.90	13.28	417	485	113	210	160	156		
	0.751	64.7	18.05	149.05	620	538	167	398	305	397	−2.89	−1.33
	0.749	70.4	19.63	82.54	477	502	117	327	215	240		
	0.748	74.4	21.19	28.18	360	440	96	250	165	171		
	0.751	82.6	23.04	18.38	338	410	90	187	112	125		
42.3 mm Circle	0.651	64.9	15.70	284.01	1294	1255	348	946	630	826	−2.89	−1.33
	0.651	69.3	16.70	157.28	906	1076	292	749	500	597		
	0.644	74.9	18.10	87.10	692	922	233	486	345	415		
	0.652	83.1	20.09	28.18	511	699	210	406	245	291		
	0.698	64.0	16.70	229.09	983	870	222	561	365	526	−2.89	−1.33
	0.693	69.4	17.90	133.86	733	795	201	494	345	411		
	0.698	73.9	19.20	70.25	566	703	182	347	200	323		
	0.706	84.1	22.10	11.93	413	478	113	201	120	156		
	0.754	64.7	18.13	141.25	604	530	167	444	335	397	−2.89	−1.33
	0.751	70.7	19.68	82.54	477	502	117	367	220	240		
	0.748	73.8	20.84	50.89	409	480	96	252	160	171		
	0.749	84.7	23.60	12.59	326	392	90	176	105	125		
37.5 mm × 37.5 mm Square	0.644	64.9	15.72	279.46	1285	1244	348	887	570	826	−2.89	−1.33
	0.657	68.2	16.50	194.98	1026	1211	292	778	510	597		
	0.648	74.3	17.90	92.29	712	948	233	460	330	415		
	0.665	84.4	20.23	23.99	503	664	210	335	225	291		
	0.701	63.6	16.60	241.73	1014	890	222	519	360	526	−2.89	−1.33
	0.699	68.5	17.90	133.86	731	796	201	460	320	411		
	0.699	74.3	19.30	68.25	559	697	182	314	180	323		
	0.703	84.6	22.10	11.93	412	534	113	184	100	156		
	0.747	63.8	17.70	165.96	655	554	167	477	345	397	−2.89	−1.33
	0.753	70.6	19.58	82.54	475	502	117	335	210	240		
	0.747	74.0	20.53	56.67	419	491	96	253	155	171		
	0.769	84.7	24.48	9.12	317	408	90	161	108	125		

Figure 13 compares the estimated ultimate bearing capacity obtained with Equation (8) and the measured the ultimate bearing capacity obtained through the model footing tests. When these graphs are examined, it is seen that the UBC, which is sometimes measured with model tests and sometimes estimated using the proposed equation, is slightly higher than the estimate value, but it is understood that these differences are within a small margin of error. It is also understood that the UBC measured at an SSD of 70% and 75% is slightly higher than the estimated value. This situation is similar to the undulating behavior of the SS both mentioned above and presented in the literature [53]. Considering the contribution of the MS values to the SS, although the MS value of the sample with an SSD of 70% is lower than the MS value of the sample with an SSD of 60%, its contribution to the SS is higher. It also appears that the size of the model foundations (i.e., 50 mm × 50 mm square; 50 mm circle; 42.3 mm circle; and 37.5 mm × 37.5 mm square) rather than the foundation shape has a limited effect on the UBC under MS.

The variation in the UBC measured according to the MS values corresponding to the SSD of 65%, 70%, 75%, 85% and 100% at three different VRs with a 50 mm diameter circular model foundation is shown in Figure 14. The results show a significant increase in UBC due to the contribution of MS in the range of the MS values corresponding to the decreasing SSD. In addition, as the VR increases, the contribution of the MS to the UBC begins to be relatively low compared to the smaller MS values.

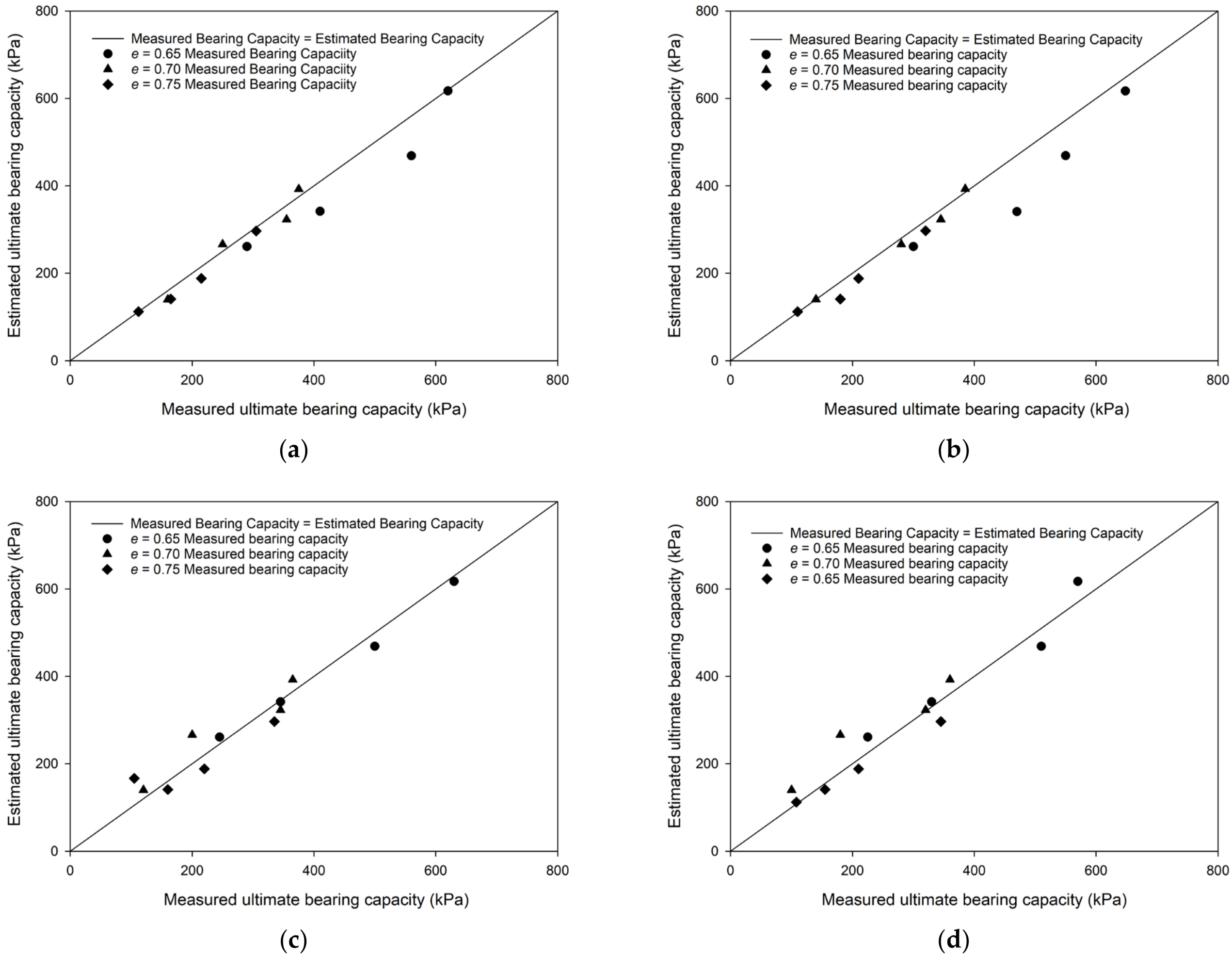

Figure 13. Comparison of the bearing capacity values found using the proposed Equation (8) and those found using the 0.1B technique: (**a**) 50 mm × 50 mm square; (**b**) 50 mm circle; (**c**) 42.3 mm circle; (**d**) 37.5 mm × 37.5 mm square.

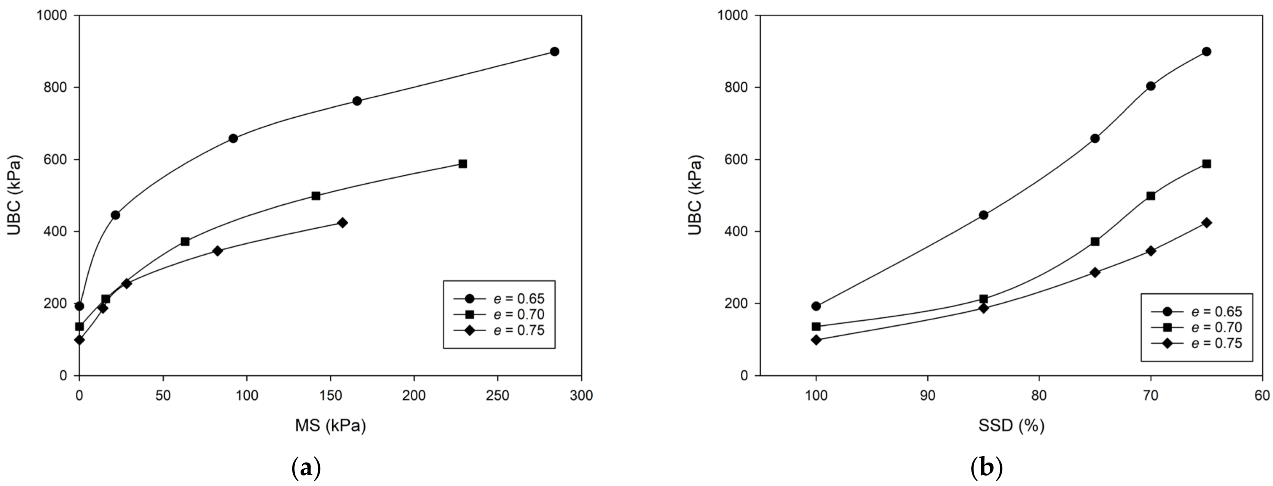

Figure 14. Graphs of 50 mm circle UBC: (**a**) MS (kPa); (**b**) SSD %.

4. Conclusions

In this study, an equation was proposed to determine the UBC of shallow foundations on unsaturated silty soil layers. In an experimental model setup created for this purpose, the UBC values of different types and sizes of model footings on silty soil layers with a different SSD/MS and VR values were measured. In addition, the SWCCs and SS parameters of unsaturated silt were determined. The conclusions obtained as a result of these experimental studies and analyses can be listed as follows:

1. Although the SS parameters of the unsaturated silty soil sample changes depending on the MS and the VR values, the failure behavior (punching failure) remains the same.
2. An increase in cohesion values in accordance with the literature was observed due to the increase in MS for all silt samples with different VRs. However, an increase was observed in the SS angle value due to the MS magnitude.
3. It was observed in the literature that the values calculated with the equations for the UBC of shallow foundations on unsaturated soils do not comply with the results of the model tests carried out on silty soils. Within the scope of this study, a new equation that gives suitable results for shallow foundations on unsaturated silty soils is proposed (Equation (8)).
4. It was determined that the foundation's UBC value for unsaturated silty soils can be estimated by using the unconfined compression test result and the fitting parameter depending on the SSD.
5. To evaluate foundations on unsaturated silty soils, the UBC can be estimated by considering the 0.1B method (ASSHTO method) by using the proposed equation in the current paper and by taking the fitting parameter (Ψ) as -2.89. If the graphical method is taken into account, the estimation can be made by taking the fitting parameter as -1.33 due to the generated relationship.
6. As the foundation size becomes smaller, the values of the foundation's UBC values measured in the model tests and calculated from the proposed equation become closer to each other. In addition, it was observed that the model foundation dimensions, and the variation in the foundation type causes changes to the measured UBC value.
7. In future studies, UBC tests can be performed on silt soils with different plasticity indexes and a relationship can be derived between the plasticity index and the fitting parameter (Ψ).

Author Contributions: Writing—original draft, M.U.Y.; conceptualization, A.O.; supervision, A.O.; investigation, M.U.Y.; methodology, M.U.Y. and A.O.; data curation, M.U.Y. and A.O.; writing—review and editing, A.O. and M.U.Y. All authors have read and agreed to the published version of the manuscript.

Funding: This research received no external funding.

Institutional Review Board Statement: Not applicable.

Informed Consent Statement: Not applicable.

Data Availability Statement: Not applicable.

Acknowledgments: We thank Sedat Sert, Ertan Bol, and Kadir Kocaman (Sakarya University) for comments and suggestions.

Conflicts of Interest: The authors declare no conflict of interest.

References

1. Terzaghi, K. *Theoretical Soil Mechanics*; John Wiley & Sons, Inc.: New York, NY, USA, 1943.
2. Skempton, A.W. The φ 0 Analysis of Stability and Its Theoretical Basis. In Proceedings of the 2nd International Conference on Soil Mechanics and Foundation Engineering (Rotterdam), Rotterdam, The Netherlands, 21–30 June 1948; pp. 72–77.
3. Meyerhof, G.G. The Ultimate Bearing Capacity of Foudations. *Geotechnique* **1951**, 2, 301–332. [CrossRef]
4. Houston, S.L.; Houston, W.N.; Wagner, A.-M. Laboratory Filter Paper Suction Measurements. *Geotech. Test. J.* **1994**, *17*, 185–194.

5. Guan, Y.; Fredlund, D.G. Use of the Tensile Strength of Water for the Direct Measurement of High Soil Suction. *Can. Geotech. J.* **1997**, *34*, 604–614. [CrossRef]
6. Houston, S.L.; Perez-Garcia, N.; Houston, W.N. Shear Strength and Shear-Induced Volume Change Behavior of Unsaturated Soils from a Triaxial Test Program. *J. Geotech. Geoenviron. Eng.* **2008**, *134*, 1619–1632. [CrossRef]
7. Bulut, R.; Wray, W.K. Free Energy of Water-Suction-in Filter Papers. *Geotech. Test. J.* **2005**, *28*, 355–364.
8. Likos, W.J.; Lu, N. Hysteresis of Capillary Stress in Unsaturated Granular Soil. *J. Eng. Mech.* **2004**, *130*, 646–655. [CrossRef]
9. Aldaood, A. Impact of Fine Materials on the Saturated and Unsaturated Behavior of Silty Sand Soil. *Ain Shams Eng. J.* **2020**, *11*, 717–725. [CrossRef]
10. Zhang, C.; Chen, X.; Fan, W.; Zhao, J. A New Unified Failure Criterion for Unsaturated Soils. *Environ. Earth Sci.* **2015**, *74*, 3345–3356. [CrossRef]
11. Yan, Q.; Zhao, J.; Zhang, C.; Wang, J. Ultimate Bearing Capacity of Strip Foundations in Unsaturated Soils Considering the Intermediate Principal Stress Effect. *Adv. Civ. Eng.* **2020**, *2020*, 8854552. [CrossRef]
12. Oloo, S.Y.; Fredlund, D.G.; Gan, J.K. Bearing Capacity of Unpaved Roads. *Can. Geotech. J.* **1997**, *34*, 398–407. [CrossRef]
13. Costa, Y.D.; Cintra, J.C.; Zornberg, J.G. Influence of Matric Suction on the Results of Plate Load Tests Performed on a Lateritic Soil Deposit. *Geotech. Test. J.* **2003**, *26*, 219–227.
14. Vanapalli, S.K.; Mohamed, F.M. Bearing Capacity of Model Footings in Unsaturated Soils. In *Experimental Unsaturated Soil Mechanics*; Springer: Berlin/Heidelberg, Germany, 2007; pp. 483–493.
15. Rojas, J.C.; Salinas, L.M.; Sejas, C. Plate-Load Tests on an Unsaturated Lean Clay. In *Experimental Unsaturated Soil Mechanics*; Springer: Berlin/Heidelberg, Germany, 2007; pp. 445–452.
16. Zhang, F.; Bao, X.; Ikariya, T. A New Model for Unsaturated Soil Using Skeleton Stress and Degree of Saturation as State Variables. *Soils Found.* **2010**, *50*, 355–370. [CrossRef]
17. Zhang, C.; Yan, Q.; Zhao, J.; Wang, J. Formulation of Ultimate Bearing Capacity for Strip Foundations Based on the Meyerhof Theory and Unsaturated Soil Mechanics. *Comput. Geotech.* **2020**, *126*, 103734. [CrossRef]
18. Oh, W.T.; Vanapalli, S.K. Interpretation of the Bearing Capacity of Unsaturated Fine-Grained Soil Using the Modified Effective and the Modified Total Stress Approaches. *Int. J. Geomech.* **2013**, *13*, 769–778. [CrossRef]
19. Ibrahim, K.M.H.I. Effect of Percentage of Low Plastic Fines on the Unsaturated Shear Strength of Compacted Gravel Soil. *Ain Shams Eng. J.* **2015**, *6*, 413–419. [CrossRef]
20. Lotfizadeh, M.R.; Kamalian, M. Estimating Bearing Capacity of Strip Footings over Two-Layered Sandy Soils Using the Characteristic Lines Method. *Int. J. Civ. Eng.* **2016**, *14*, 107–116. [CrossRef]
21. Maghvan, S.V.; Imam, R.; McCartney, J.S. Relative Density Effects on the Bearing Capacity of Unsaturated Sand. *Soils Found.* **2019**, *59*, 1280–1291. [CrossRef]
22. Chen, T.; Xiao, S. An Upper Bound Solution to Undrained Bearing Capacity of Rigid Strip Footings Near Slopes. *Int. J. Civ. Eng.* **2020**, *18*, 475–485. [CrossRef]
23. Chen, W.; Xia, W.; Zhang, S.; Wang, E. Study on the Influence of Groundwater Variation on the Bearing Capacity of Sandy Shallow Foundation. *Appl. Sci.* **2023**, *13*, 473. [CrossRef]
24. Silveira, I.A.; Rodrigues, R.A. Collapsible Behavior of Lateritic Soil Due to Compacting Conditions. *Int. J. Civ. Eng.* **2020**, *18*, 1157–1166. [CrossRef]
25. Liu, Y.; Vanapalli, S.K. Mechanical Behavior of a Floating Model Pile in Unsaturated Expansive Soil Associated with Water Infiltration: Laboratory Investigations and Numerical Simulations. *Soils Found.* **2021**, *61*, 929–943. [CrossRef]
26. Tan, M.; Cheng, X.; Vanapalli, S. Simple Approaches for the Design of Shallow and Deep Foundations for Unsaturated Soils I: Theoretical and Experimental Studies. *Indian Geotech. J.* **2021**, *51*, 97–114. [CrossRef]
27. Tan, M.; Vanapalli, S.K. Foundation Bearing Capacity Estimation on Unsaturated Soil Slope under Transient Flow Condition Using Slip Line Method. *Comput. Geotech.* **2022**, *148*, 104804. [CrossRef]
28. Vanapalli, S.K.; Salinas, L.M.; Avila, D.; Karube, D. Suction and Storage Characteristics of Unsaturated Soils. In *Unsaturated Soils-Volume 3: Proceedings of the 3rd International Conference on Unsaturated Soils, UNSAT 2002, 10–13 March 2002, Recife, Brazil*; CRC Press: Boca Raton, FL, USA, 2021; p. 1045.
29. Cheng, Y.-Y.; Gao, X.-G.; Liu, T.-H.; Li, L.-X.; Du, W.; Hamad, A.; Wang, J.-P. Effect of Water Content on Strength of Alluvial Silt in The Lower Yellow River. *Water* **2022**, *14*, 3231. [CrossRef]
30. Fredlund, D.G.; Morgenstern, N.R. Stress State Variables for Unsaturated Soils. *J. Geotech. Eng. Div.* **1977**, *103*, 447–466. [CrossRef]
31. Oh, W.T.; Vanapalli, S.K. Modelling the Applied Vertical Stress and Settlement Relationship of Shallow Foundations in Saturated and Unsaturated Sands. *Can. Geotech. J.* **2011**, *48*, 425–438. [CrossRef]
32. Vahedifard, F.; Robinson, J.D. Unified Method for Estimating the Ultimate Bearing Capacity of Shallow Foundations in Variably Saturated Soils under Steady Flow. *J. Geotech. Geoenviron. Eng.* **2016**, *142*, 04015095. [CrossRef]
33. Vo, T.; Russell, A.R. Bearing Capacity of Strip Footings on Unsaturated Soils by the Slip Line Theory. *Comput. Geotech.* **2016**, *74*, 122–131. [CrossRef]
34. Oh, W.T.; Vanapalli, S.K. Modeling the Stress versus Settlement Behavior of Shallow Foundations in Unsaturated Cohesive Soils Extending the Modified Total Stress Approach. *Soils Found.* **2018**, *58*, 382–397. [CrossRef]
35. Ghasemzadeh, H.; Akbari, F. Determining the Bearing Capacity Factor Due to Nonlinear Matric Suction Distribution in the Soil. *Can. J. Soil Sci.* **2019**, *99*, 434–446. [CrossRef]

36. Ghasemzadeh, H.; Akbari, F. Investigation of Soil Active Wedge Angle with Linear Matric Suction Distribution below the Footing. *Int. J. Civ. Eng.* **2020**, *18*, 161–168. [CrossRef]
37. Akbari Garakani, A.; Sadeghi, H.; Saheb, S.; Lamei, A. Bearing Capacity of Shallow Foundations on Unsaturated Soils: Analytical Approach with 3D Numerical Simulations and Experimental Validations. *Int. J. Geomech.* **2020**, *20*, 04019181. [CrossRef]
38. Lu, N.; Godt, J.W.; Wu, D.T. A Closed-Form Equation for Effective Stress in Unsaturated Soil. *Water Resour. Res.* **2010**, *46*, W05515. [CrossRef]
39. Griffiths, D.V.; Lu, N. Unsaturated Slope Stability Analysis with Steady Infiltration or Evaporation Using Elasto-Plastic Finite Elements. *Int. J. Numer. Anal. Methods Geomech.* **2005**, *29*, 249–267. [CrossRef]
40. Zhang, L.L.; Fredlund, D.G.; Fredlund, M.D.; Wilson, G.W. Modeling the Unsaturated Soil Zone in Slope Stability Analysis. *Can. Geotech. J.* **2014**, *51*, 1384–1398. [CrossRef]
41. Consoli, N.C.; Schnaid, F.; Milititsky, J. Interpretation of Plate Load Tests on Residual Soil Site. *J. Geotech. Geoenviron. Eng.* **1998**, *124*, 857–867. [CrossRef]
42. Tang, Y.; Taiebat, H.A.; Russell, A.R. Bearing Capacity of Shallow Foundations in Unsaturated Soil Considering Hydraulic Hysteresis and Three Drainage Conditions. *Int. J. Geomech.* **2017**, *17*, 04016142. [CrossRef]
43. Meyerhof, G.G. Some Recent Research on the Bearing Capacity of Foundations. *Can. Geotech. J.* **1963**, *1*, 16–26. [CrossRef]
44. Vesić, A.S. Analysis of Ultimate Loads of Shallow Foundations. *J. Soil Mech. Found. Div.* **1973**, *99*, 45–73. [CrossRef]
45. Kumbhojkar, A.S. Numerical Evaluation of Terzaghi's N γ. *J. Geotech. Eng.* **1993**, *119*, 598–607. [CrossRef]
46. Gan, J.K.M.; Fredlund, D.G.; Rahardjo, H. Determination of the Shear Strength Parameters of an Unsaturated Soil Using the Direct Shear Test. *Can. Geotech. J.* **1988**, *25*, 500–510. [CrossRef]
47. Escario, V.; Saez, J. The Shear Strength of Partly Saturated Soils. *Geotechnique* **1986**, *36*, 453–456. [CrossRef]
48. Vanapalli, S.K.; Fredlund, D.G.; Pufahl, D.E. The Relationship between the Soil-Water Characteristic Curve and the Unsaturated Shear Strength of a Compacted Glacial Till. *Geotech. Test. J.* **1996**, *19*, 259–268.
49. *ASTM D4318-17e1*; Standard Test Methods for Liquid Limit, Plastic Limit, and Plasticity Index of Soils. ASTM International: West Conshohocken, PA, USA, 2010.
50. Kruse, G.A.; Dijkstra, T.A.; Schokking, F. Effects of Soil Structure on Soil Behaviour: Illustrated with Loess, Glacially Loaded Clay and Simulated Flaser Bedding Examples. *Eng. Geol.* **2007**, *91*, 34–45. [CrossRef]
51. Ltifi, M.; Abichou, T.; Tisot, J.P. Effects of Soil Aging on Mechanical and Hydraulic Properties of a Silty Soil. *Geotech. Geol. Eng.* **2014**, *32*, 1101–1108. [CrossRef]
52. Dijkstra, T.A.; Rogers, C.D.F.; Smalley, I.J.; Derbyshire, E.; Li, Y.J.; Meng, X.M. The Loess of North-Central China: Geotechnical Properties and Their Relation to Slope Stability. *Eng. Geol.* **1994**, *36*, 153–171. [CrossRef]
53. Wen, B.-P.; Yan, Y.-J. Influence of Structure on Shear Characteristics of the Unsaturated Loess in Lanzhou, China. *Eng. Geol.* **2014**, *168*, 46–58. [CrossRef]
54. Önalp, A.; Arel, E.; Bol, E.; Özocak, A.; Sert, S. *The Assessment of Liquefaction Potential with Dissipation Method in Piezocone Penetration Testing (CPTU)*; Scientific and Technological Research Council of Turkey: Ankara, Türkiye, 2007.
55. Fredlund, D.G.; Rahardjo, H. *Soil Mechanics for Unsaturated Soils*; John Wiley & Sons: Hoboken, NJ, USA, 1993.
56. Hu, Z.Q.; Shen, Z.J.; Xie, D.Y. Research on Structural Behavior of Unsaturated Loess. *Chin. J. Rock Mech. Eng.* **2000**, *19*, 775–779.
57. Maleki, M.; Bayat, M. Experimental Evaluation of Mechanical Behavior of Unsaturated Silty Sand under Constant Water Content Condition. *Eng. Geol.* **2012**, *141*, 45–56. [CrossRef]
58. Oloo, S.Y.; Fredlund, D.G. A Method for Determination of φ b for Statically Compacted Soils. *Can. Geotech. J.* **1996**, *33*, 272–280. [CrossRef]
59. Vanapalli, S.K.; Fredlund, D.G. Comparison of Different Procedures to Predict Unsaturated Soil Shear Strength. *Geotech. Spec. Publ.* **2000**, *99*, 195–209.
60. Vanapalli, S.K.; Lane, J.J. A Simple Technique for Determining the Shear Strength of Finegrained Unsaturated Soils Using the Conventional Direct Shear Apparatus. In Proceedings of the Second Canadian Specialty Conference on Computer Applications in Geotechnique, Winnipeg, Canada; Citeseer. 2002; pp. 245–253.
61. Gardner, R. A Method of Measuring the Capillary Tension of Soil Moisture over a Wide Moisture Range. *Soil Sci.* **1937**, *43*, 277–284. [CrossRef]
62. Qian, J.S.; Lu, H. Effect of Compaction Degree on Soil-Water Characteristic Curve of Chongming Clay. In *Applied Mechanics and Materials*; Trans Tech Publications Ltd.: Wollerau, Switzerland, 2011; Volume 90, pp. 701–706.
63. *ASTM D5298-16*; Standard Test Method for Measurement of Soil Potential (Suction) Using Filter Paper. ASTM International: West Conshohocken, PA, USA, 2016.
64. Hilf, J.W. *An Investigation of Pore-Water Pressure in Compacted Cohesive Soils*; University of Colorado at Boulder: Boulder, CO, USA, 1956.
65. Cresswell, H.P.; Green, T.W.; McKenzie, N.J. The Adequacy of Pressure Plate Apparatus for Determining Soil Water Retention. *Soil Sci. Soc. Am. J.* **2008**, *72*, 41–49. [CrossRef]
66. Adams, M.T.; Collin, J.G. Large Model Spread Footing Load Tests on Geosynthetic Reinforced Soil Foundations. *J. Geotech. Geoenviron. Eng.* **1997**, *123*, 66–72. [CrossRef]
67. Oh, W.T.; Garga, V.K.; Vanapalli, S.K. Shear Strength Characteristics of Statically Compacted Unsaturated Kaolin. *Can. Geotech. J.* **2008**, *45*, 910–922. [CrossRef]

68. Oloo, S.Y. *A Bearing Capacity Approach to the Design of Low-Volume Traffic Roads*; University of Saskatchewan: Saskatoon, SK, Canada, 1999.
69. *ASTM D3080-04*; Standard Test Method for Direct Shear Test of Soils under Consolidated Drained Conditions. ASTM International: West Conshohocken, PA, USA, 1999.
70. Van Genuchten, M.T. A Closed-Form Equation for Predicting the Hydraulic Conductivity of Unsaturated Soils. *Soil Sci. Soc. Am. J.* **1980**, *44*, 892–898. [CrossRef]
71. *ASTM D1194-94*; Standard Test Method for Bearing Capacity of Soil for Static Load and Spread Footings. ASTM International: West Conshohocken, PA, USA, 2003.
72. Steensen-Bach, J.O.; Foged, N.; Steenfelt, J.S. Capillary Induced Stresses—fact or Fiction? In Proceedings of the 9th European Conference on Soil Mechanics and foundation Engineering, Dublin, Ireland, 31 August–3 September 1987; pp. 83–89.